

Spatial and temporal relations between magnetic elements and bright points in the photospheric network

R. Muller¹, A. Dollfus³, M. Montagne², J. Moity³, and J. Vigneau²

¹ Observatoire du Pic du Midi, BP 136, 65201 Bagnères de Bigorre, France

² Observatoire Midi-Pyrénées, 14 Avenue Edouard Belin, 31400 Toulouse, France

³ Observatoire de Meudon, DASOP, 92195 Meudon Cedex, France

Received 3 June 1998 / Accepted 20 January 2000

Abstract. 28 min time series of high resolution magnetograms, continuum filtergrams and line core filtergrams have been obtained in the line FeI 6173, with the 50 cm refractor of the Pic du Midi Observatory, in a quiet area near the solar disk center. Their comparison shows that every bright point of the photospheric network coincides better than 0''5 with a magnetic element of small size (smaller than 1''). The maximum of magnetic field strength of a magnetic element does not necessarily occur at the same time as the maximum of brightness. Such spatial and temporal relations cannot be explained by static models of flux tubes, but they can be by a dynamic flux tube model, as computed by Steiner et al. (1996). The observations also show that a magnetic element present in the network becomes bright and forms a bright point when it is compressed by the surrounding granules as they converge. This is an indication that the dynamics of granulation plays a major role in the concentration of the magnetic field into thin flux tubes, near the surface of the Sun.

Key words: Sun: granulation – Sun: magnetic fields – Sun: photosphere

1. Introduction

The magnetic field in solar faculae, as well as in the photospheric network away from active regions, is made of thin flux tubes of high field strength, 1 to 2 kG, with a small cross section (lower than 300 km). The high field strength and the small scale were first inferred from low resolution observations and indirect methods (Stenflo, 1973). Soon after, a pattern of very small bright points (the solar filigree), corresponding to the magnetic network, was discovered by Dunn & Zirker (1973), in high resolution H α filtergrams. Their observations have revealed that the bright points are located in the dark lanes between granules, and that their size is smaller than 0''3 (200 km), confirming Stenflo's expectations. The existence of kilogauss field strengths located in small-scale magnetic elements was confirmed later on, with the help of high resolution spectrograms and magnetograms taken in the visible range (Chapman 1974; Tarbell & Title 1977; Koutchmy & Stellmacher 1978; Del Toro Iniesta et al. 1990; Keller et al. 1990; Title et al. 1992; Stolpe & Kneer

1997). Direct measurements of kG fields were also achieved in the IR range, where photospheric lines are fully splitted by the Zeeman effect (Harvey & Hall 1975; Stenflo et al. 1987; Solanki et al. 1989; Zayer et al. 1989; Zayer 1990; Muglach & Solanki 1992).

Only recently, it has been shown that the sizes of the magnetic elements (the extension of the magnetic signal in magnetograms) and of the associated bright points are nearly the same, owing to very high resolution magnetograms (0''3) obtained with narrowband birefringent filters tuned to the wings of photospheric lines (Keller 1992; Berger & Title 1996; Scharmer 1996). However, because time series of high resolution magnetograms were not available yet, most information about the dynamical behaviour of the small scale magnetic elements have been derived from high resolution time sequences of wide-band filtergrams, where they appear as bright points, which we call Network Bright Points or NBPs. The observations were taken in white light (Muller 1983; Muller & Roudier 1992; Roudier et al. 1994; Muller et al. 1994), or in the G-Band of the CH molecule, at 4307 Å (Muller 1985; Muller & Mena 1987; Berger et al. 1995; Berger & Title 1996). It is very easy to identify the magnetic elements in G-band images, because they appear very bright compared to their dark intergranular surrounding; often they are even brighter than the neighbouring granules (Title & Berger 1996). In the white-light observations used by Muller (1983), the magnetic elements have been identified with help of quasi-simultaneous filtergrams taken with a 15 Å bandpass filter centered in the CaII 3933 Å Fraunhofer line, where they also show up brighter than the surrounding photosphere. In the subsequent papers by Muller & Roudier (1992) and Roudier et al. (1994), NBPs were directly identified in the white light time series without the help of G-band or calcium images, thanks to some peculiar characteristics (small size, high sharpness, long lifetime) which allows us to make an easy differentiation with the smallest granules.

All the investigations quoted above show that the evolution of the NBPs is dominated by the dynamical behavior of the neighbouring granules. They form in intergranular spaces, at the junction of converging granules (Muller 1983; Muller & Roudier 1992); they split when they are squeezed between two granules, but they can also merge (Muller 1983; Roudier

& Muller 1994; Berger & Title 1996). NBPs thus appear as unstable features; however the two groups of authors did not find the same degree of instability: according to Berger and Title, the evolution timescale is of about the time scale of granulation, 6 to 8 minutes typically; on the contrary, Muller and Roudier found the bright elements more stable, experiencing much less fragmentations and mergings than reported by Berger and Title, and having an average lifetime of 16 minutes (the lifetime of a few NBPs was found to be as long as 50 minutes). The difference may come from a better resolution in the G-band images at 4307 Å than in the white-light images at 5750 Å, or to the fact that Muller and Roudier investigated a quieter region than Berger and Title. On the other hand, the criteria in the visual identification used by the Pic du Midi group may be different from those of the numerical algorithms used by the Lockheed group.

The models which best explain the properties of bright points (continuum contrast and its center-to-limb variation, I and V Stokes- profiles of photospheric lines) imply thin, evacuated flux tubes, and were first introduced by Spruit (1976). They have been improved over the years (Deinzer et al. 1984; Steiner et al. 1986; Knölker et al. 1988; Knölker & Schüssler 1988; Grossmann-Doerth et al. 1989; Steiner & Pizzo 1989; Pizzo et al. 1993a; 1993b; Grossmann-Doerth et al. 1994; Steiner et al. 1995; 1996; 1998). The magnetic field blocks a part of the heat flux from below, making sunspots and pores to appear darker than the photosphere. In the case of flux tubes of small cross-section, not larger than about 300 km, the hot walls and the deeper layers shine and heat the gas of the upper layers inside the tubes. Consequently, they appear brighter than the average photosphere, even at disk center. Larger flux tubes should be dark.

These theoretical predictions about the size-brightness relation have been first supported by the observational results of Spruit & Zwaan (1981) who, analysing Calcium-K filtergrams, concluded that the elements smaller than 0''5 (360 km) are brighter than the average photosphere, while those larger than 1''6 (1200 km) correspond to pores; furthermore they suggested that in the intermediate range of sizes (0''5 to 1''6), the elements are not brighter nor darker than average, which means that they cannot be easily identified in filtergrams. It was only recently that these predictions have also been verified directly in high resolution magnetograms, obtained with the help a speckle technique, by Keller (1992, 1995). This author actually found that magnetic elements larger than 300 km correspond to areas darker than the average in the granulation pattern. Subsequently, direct (not restored) high-resolution magnetograms have been obtained, confirming that every bright point visible either in the continuum or in photospheric line-core filtergrams (Title et al. 1992; Yi & Engvold 1993) or in G-band filtergrams (Berger & Title 1996), is associated with a magnetic element. Sometimes, however, a magnetic element can be found, which is not associated with a bright point. When a magnetic element is seen as a single, isolated feature, it has nearly the same size as the associated bright point. But, surprisingly, when several bright points are close together, they appear inside a large magnetic feature,

covering an area which may extend well beyond the points (see, for example, Figs. 7 and 8 in Keller, 1995).

The aim of this work is to study in more details the spatial and the temporal relations between magnetic elements and the associated bright points, in order to understand better the role played by the granulation in the magnetic field concentration process. It appears that the results are difficult to explain with a model of static evacuated flux tube, of Spruit's type; however they can well be explained by the recent dynamical model of Steiner et al. (1996). Our investigation was made in the photospheric network, away from active regions, because there, the magnetic elements appear much more isolated, making easier to understand the interaction between granulation and magnetic fields.

The observations will be described in Sect. 2, and the technique to get the magnetograms in Sect. 3. The results will be presented in Sect. 4 and discussed in Sect. 5.

2. Observations

The observations were made with the 50-cm refractor of the Pic du Midi Observatory, under excellent seeing conditions, on March the 23rd, 1995. The solar magnetograph using a Lyot-type monochromatic filter, designed by A. Dollfus (Dollfus et al., 1985) and previously used at the Meudon Observatory (Dollfus et al. 1986; Dollfus 1990; Dollfus & Moity 1992), has been installed behind the prime focus of the Pic du Midi refractor. It includes a polarization analyser allowing the measurement of the V , U and Q Stokes signals produced by the solar magnetic field. This polarization analyser is aligned on the optical axis of the refractor, before the monochromatic filter and any mirror, in order to minimize the level of the instrumental polarization. Because the instrument is a refractor, this level should be negligible.

In the present observations only the longitudinal magnetic field of solar features was measured. The circularly polarized light was transformed into linearly polarized light by a $\lambda/4$ plate followed by a polarizing device (Rochon prism), so that only the light due to one circular Zeeman component enters the narrow-band filter. The other Zeeman component is allowed to replace the first one in less than 0.1 s, by rotating the $\lambda/4$ plate by 90° .

The bandpass of the monochromatic filter is 0.15 Å at λ 6173 (in fact the filter consists of two birefringent units: a pre-filter with a bandpass 0.6 Å, followed by a narrowband unit of 0.15 Å). We have selected the spectral line FeI 6173 (Landé factor $g = 2.5$) because it is well isolated: a clean continuum on each side of the line helps putting the bandpass of the filter precisely in the core, or symmetrically in each wing. In its nominal configuration, the filter is centred on the core of the line and its bandpass is symmetrical, including two weak side-lobes. The bandpass can be shifted in less than 0.1 s to one of the wings of the photospheric line, by rotating a $\lambda/4$ plate by $\pm 45^\circ$. In this case the bandpass of the filter is no longer symmetrical, because one of the side-lobes increases (see, for more details, Dollfus et al. 1985). When the $\lambda/4$ plate is rotated by 90° , the bandpass of the filter is composed of two symmetric lobes, while the central

component has disappeared; these two lobes are positioned in the continuum, on each side of the photospheric line. Thus, rotating a $\lambda/4$ plate, one can make, as fast as permitted by the acquisition rate of the camera, four observations at various positions in a photospheric line: in the line core, in the blue and red wings, and in the adjacent continuum. Furthermore, the circular polarization analyser allows to take the images alternatively in the two, left and right, circular polarizations, in the wings of the line, and then to get longitudinal field magnetograms.

The observations used in this work, were made in a quiet area of the Sun, near disk center, away from any active region. The seeing was excellent. The detector was a fast movie camera (a fast CCD camera is now available). The instrument was used with a f/50 ratio, which offers a good compromise between a short enough exposure time (1/10 sec) and an acceptable film granularity (which limits the polarimetric sensitivity).

Our observation lasted 45 minutes and was divided into a number of repeated cycles. An observing cycle consisted of 6 bursts taken sequentially: line core, continuum, blue wing (two polarizations), and red wing (two polarizations). In each burst (i.e. for any given bandpass position and polarization state), 16 frames were taken at a rate of 4 frames per second, in order to increase the probability to get a large number of good pictures. The exposure time was 0.1 s and the duration of a cycle 70 s in average. These cycles were repeated all along the 45 minutes duration of the observation.

3. Image processing and creation of magnetograms

3.1. Digitization

We have selected the best 28 minutes from the 45 minutes of observation. Thus 23 cycles of 6 bursts, each containing 16 frames, i.e. about 2200 frames have been digitized with the MAMA (Machine A Mesurer les images Astronomiques) in the Center for Images Analysis at Paris Observatory. The size of the digitized frames was 1024×1536 square pixels of $20 \mu\text{m}$ ($0''.16$). We have selected a subarea of 600×600 pixels ($96'' \times 96''$), where several groups of Network Bright Points are visible in the line core, in order to reduce the computer time. Film densities have been converted into intensities relative to the average photosphere with the help of the film calibration curve.

3.2. Frames alignment and image destretching

During the observation, the seeing was stable enough to select about a dozen best frames in each burst. All these selected best frames in a same burst are aligned and destretched relatively to a reference frame, then added in order to decrease the noise and increase the signal to noise ratio, making easier the magnetic elements detection. Three time series, respectively for continuum, line core and magnetic field, are thus obtained, each made of 23 images corresponding to the 23 selected cycles.

In order to follow the evolution of the fine structures along the series of images, the 23 continuum filtergrams are aligned and destretched: the second is referred to the first, the third to the

second, and so on. Because the features in magnetograms are of different nature than in continuum filtergrams, they cannot be directly correlated for alignment. To overcome this problem, the cross-correlations were computed between continuum filtergrams and one of the two polarized images in a wing, which look rather similar. The accuracy of the full frame alignments is better than $0''.1$.

For correcting the time varying atmospheric distortion, we have adapted a “destretching” code developed by L. November (1986). Each frame is divided in subframes: a vector-displacement is computed for each of them; then, for each point in the field of view, a vector-displacement is computed by interpolating the vectors of the surrounding subareas. The best results are obtained with a grid of 15×15 subframes of 40×40 pixels ($6.5'' \times 6.5''$) in size, and two iterations. The field of $6.5''$ can be considered as the size of the isoplanatic patch in our observations.

Both destretching and frame superposition slightly smooth the features in the images. Because film granularity is more affected than the magnetic elements, due to their relative dimensions, the signal to noise ratio is improved.

3.3. Creation of magnetograms

A longitudinal magnetogram is made from the classical combination of images taken in opposite circular polarizations, I^+ and I^- , in the same line wing:

$$P = [I^+ - I^-]/[I^+ + I^-] = V/I$$

where P is the polarization signal, while V and I are the Stokes parameters. As said in the previous section, each I^+ and I^- image is the sum of about a dozen of individual frames, aligned and destretched relatively to the same reference. However, the average blurring and distortion in the two composite images, I^+ and I^- , are not exactly identical. This results in a residual noise in the differential image, which becomes more critical when the spatial resolution increases. It thus appears that a precise destretching is necessary to make high resolution and high signal to noise magnetograms on a large field.

When the seeing quality is not quite identical in the two polarized images (quantified by the root mean square, rms, of the intensity fluctuations), we then slightly smooth the best image, which significantly improves the signal to noise ratio in the differential image. This differential image is also improved by using the observations taken in the blue wing of the photospheric line, where the granulation contrast is lower than in the red wing.

3.4. Line and core continuum filtergrams

The line core and continuum filtergrams are also made by summing about a dozen of individual aligned and destretched frames. In such a way, the photographic noise is reduced, and the bright points in the filtergrams are similarly smeared by atmospheric blurring and image processing as the associated magnetic elements in the magnetograms. The connection be-

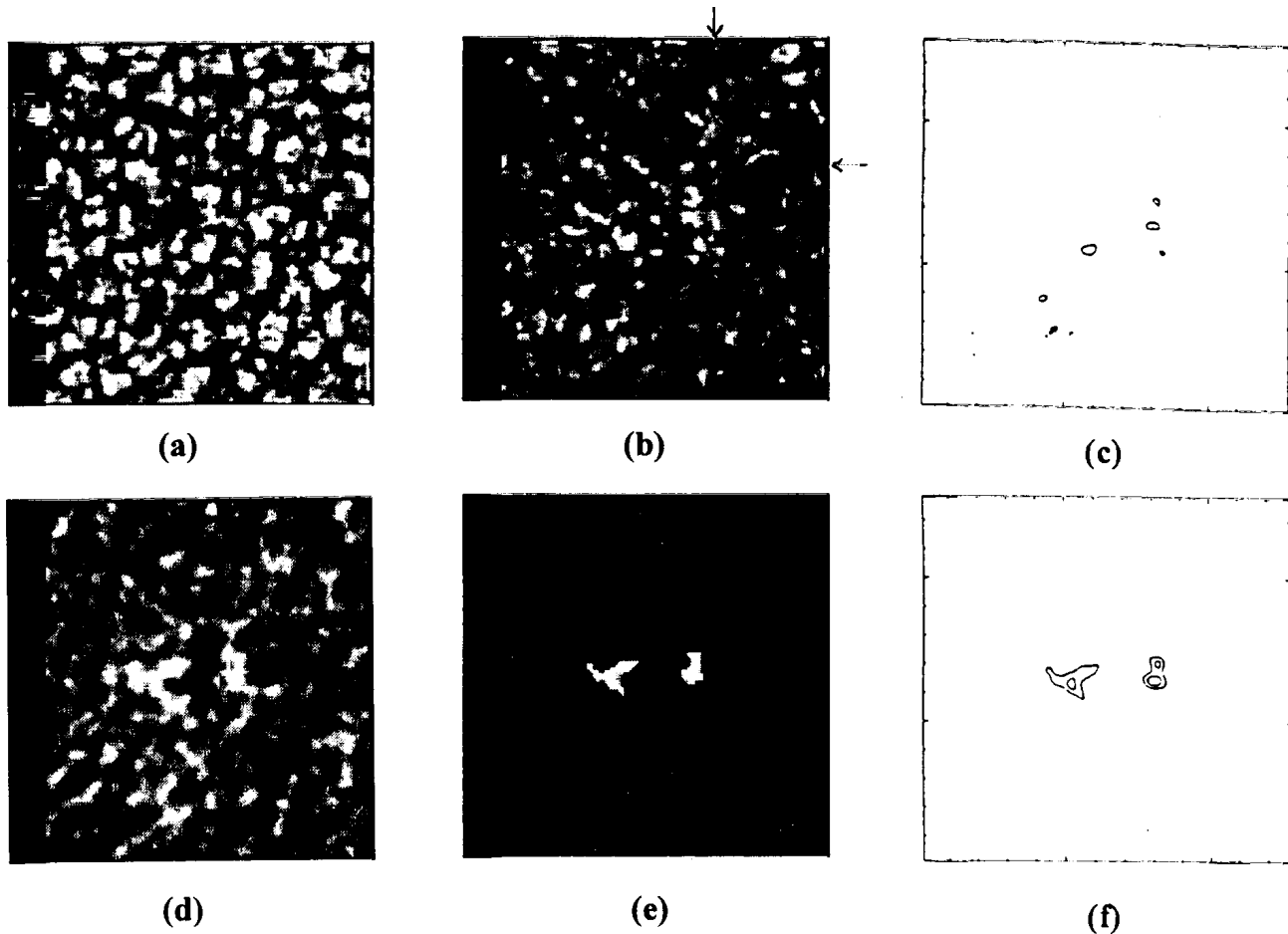


Fig. 1a–e. Analysis of a $20'' \times 20''$ quiet area at the solar disk center: **a** Continuum filtergram showing the granular pattern. **b** Line core filtergram showing the bright points. The smallest one is located by tick marks. **c** Intensity isophotes from **b**, at level 1.10 above the mean. **d** Longitudinal field magnetogram showing the magnetic areas in bright. **e** The same as **d** with a 3σ threshold. **f** Isophotes from **e**, corresponding to 0.75% and 1% polarization signal

tween features seen in magnetograms and filtergrams can thus be made reliably.

4. Description of filtergrams and magnetograms

4.1. Continuum filtergrams

It is of course the granular pattern which is visible in the continuum filtergrams: Fig. 1a presents such a filtergram for a square area $20'' \times 20''$. However, the fine structure (narrow lanes) one should see in the largest granules does not show up, nor small granules which should be visible in large number. The rms of the granulation intensity fluctuation is 2.5 to 3%; it should be of 6 to 7% at 6173 \AA , when observed with a nearly perfect 50 cm refractor under excellent seeing conditions. In addition to the unavoidable diffraction of the telescope, a source of contrast lost is the light scattered by the Lyot filter. Some additional smearing comes from the destretching, as explained above, and because numerical filters have been applied to the images in order to smooth the noise. The line core filtergrams and the magnetograms described below, are similarly smeared, explaining

the low contrast and the relatively weak magnetic signal of the magnetic elements.

4.2. Line core filtergrams

The core of FeI 6173 forms in layers 200 to 300 km above the surface, where the granulation contrast vanishes or even is inverted (Deubner 1989; Espagnet et al. 1995; Stein & Nordlund 1989). Because the width of the Lyot filter bandpass (0.15 \AA) is of the same order as the line width, it allows for a significant contribution from the lower photospheric layers in our line core filtergrams, and the granulation pattern is still visible, with nearly the same contrast as in the continuum filtergrams. An example is given in Fig. 1b, for the same area as in Fig. 1a.

Several groups of small bright points show up against the granulation pattern: they are Network Bright Points (NBPs), as confirmed by the detection of associated magnetic fluxes (Sect. 4.3) and by their lifetime which is much longer than 10 minutes, the average lifetime of granules (see Muller & Roudier, 1992, for NBPs identification). Their brightness, relative to the

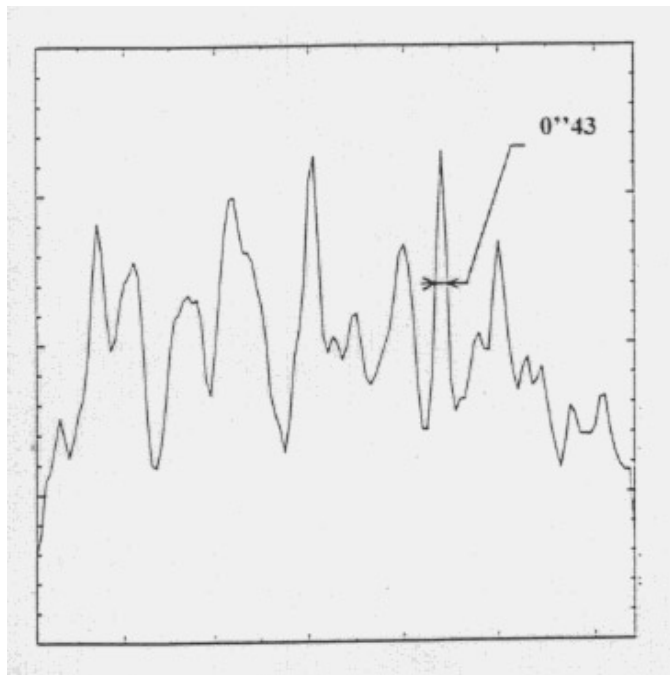


Fig. 2. Photometric cut along the line in (1b) diametrically crossing the marked NBP

average photosphere transmitted by the filter does not exceed 1.15, as shown in Fig. 1c by their isophotes lying 1.10 above the mean intensity of the area. The smallest identified NBP is shown by tick marks in Fig. 1b. Fig. 2 presents the photometric cut of the corresponding line on which is measured the width at half-maximum of the pic associated with this NBP: $0''43$. In the best filtergrams published in the literature, the smallest NBPs are nearly diffraction limited in size, between $0''30$ and $0''20$, depending on the telescope aperture and the filter wavelength (Dunn & Zirker 1973; Mehlretter 1974; Koutchmy 1977; Muller & Keil 1983; Auffret & Muller 1990; Berger et al. 1995).

4.3. Longitudinal field magnetograms

Several magnetic areas appear in the field of view (bright areas in Fig. 1d) above a noise pattern which will be discussed below. They all correspond to groups of NBPs visible in line core filtergrams as shown in Figs. 3a and 3d, in which they have been encircled. They persist over the 28 minutes time sequence. The strongest polarization signal V/I measured in our observations is 2.2%: Fig. 1f shows isophotes of the magnetogram 1d, corresponding to 0.75% and 1% polarization signal. For a 1000 Gauss longitudinal field strength, the calibration of our device indicates that this polarization signal should be about 6%, when measured with an infinite resolution telescope. Keller (1992) detected a signal of 8% in one NBP on a $0.3''$ resolution magnetogram obtained after restoration by speckle technique. The rms of the intensity fluctuations in the noise pattern, outside the magnetic elements, is equivalent to a signal of 0.25%. These fluctuations are due in part to the granularity of the film,

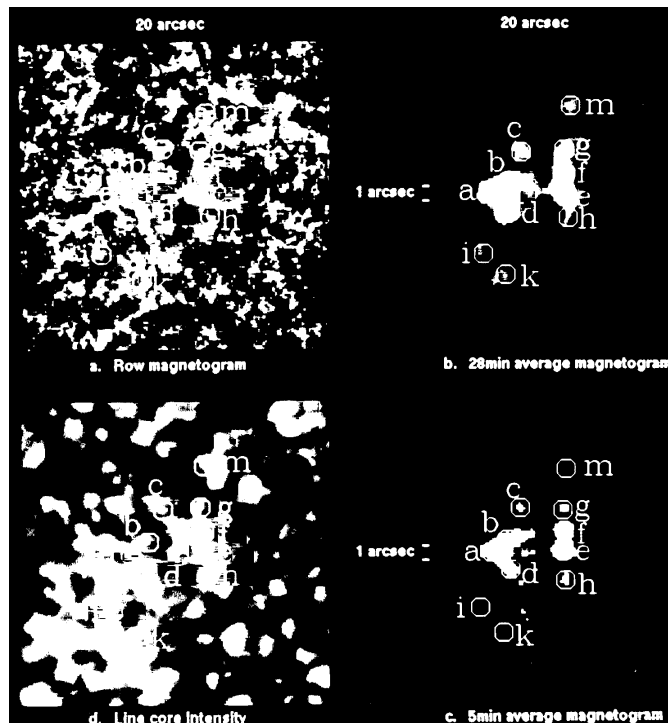


Fig. 3a – d. Magnetograms **a**, **b**, **c** and line core filtergram **d** of the same area as in Fig. 1, but not obtained at the same time, and showing several identified magnetic elements. In the magnetograms **b**, **c**, only the areas with a polarization signal larger than 0.75% (3σ) are shown

but mainly to mismatch effects in the subtraction of images of opposite polarities, which were not taken simultaneously. For example, with 10% contrast between a granule and its adjacent dark lane over a distance of $1''$, and with $0.1''$ misalignment between the two polarization images, a 1% spurious signal will appear.

In order to improve the identification of the magnetic elements, the magnetograms have been “thresholded” to $2.5\sigma = 0.63\%$ of polarization signal. This value 2.5σ was chosen because it is a compromise between a 3σ threshold (as shown in Fig. 1e), for which not only most of the noise pattern is removed, but also some magnetic signal, and a 2σ threshold, for which the magnetograms remain too much noisy. Such “thresholded” magnetograms contain magnetic elements as well as some small size artefacts. Fortunately, the two kinds of elements can be distinguished in the time series: the first ones are persistent in successive magnetograms, the second ones are not. When one averages the 23 magnetograms (keeping the 2.5σ threshold), the noise is washed out and only the magnetic elements remain visible.

Eleven magnetic elements are identified in the $20'' \times 20''$ area of the quiet Sun shown in Fig. 3b. They appear either as isolated features or inside two small permanent magnetic areas, 2 to 4 arcsecond in size. In these areas, 3 to 4 elements were evolving during the 28 minutes observed sequence. Their time evolution is better analysed in a series of running mean magnetograms obtained by averaging 4 consecutive individual magnetograms,

thus producing 5 minutes averaged magnetograms, such as in Fig. 3c. The time interval between consecutive mean magnetograms is 1 mn 13 s in average. All these elements are associated to bright points in line core filtergrams (Fig. 3d), confirming the close association between NBPs and magnetic fields. All the magnetic elements detected in the small $20'' \times 20''$ investigated field, have the same polarity.

Because the instrumental response makes the Stokes V signal under-estimated, transformation of this polarization signal into a magnetic field strength is meaningless.

5. Results and discussion: spatial and temporal relations between magnetic elements and network bright points

In the presentation of the results which follows, the isolated elements will be distinguished from those which appear in groups.

Concerning the **isolated elements**, there is a close spatial relation between the magnetic elements and the corresponding bright points visible in the line core filtergrams. The sizes of the bright points are in the range $0''.4 - 1''$. The observed sizes of the corresponding magnetic features depend on the threshold used: for a 2.5σ threshold, it is of the same order, not exceeding $1''$. One can conclude that the magnetic flux does not extend much more than the associated brightening. The spatial coincidence is often not perfect, but is usually better than $0''.5$. A part of the shift is due to a local residual misalignment between filtergrams and the corresponding magnetograms; however, we checked that shifts as large as $0''.5$ cannot be explained by the processing alone. That means that at least a part of the shift should be real.

When one compares a magnetogram with the filtergram taken nearly at the same time, one can find a few magnetic elements without corresponding bright points and conversely, although they are not always visible at the same time. But when one looks at the time series one sees that a bright point corresponds to every detected magnetic element, and conversely. Our results thus confirm previous findings about the relation between magnetic field and brightness, all based on the comparison of a single pair of frames (Keller 1992, 1995; Title et al. 1992; Yi & Engvold 1993; Berger & Title 1996; Scharmer 1996).

In addition, we find that the time of maximum longitudinal field strength does not necessarily coincides with the time of maximum brightness. One must take care however that, sometimes, the magnetic signal may weaken or cannot be detected because of seeing degradation. We also see a tendency for the magnetic flux to appear before the associated bright point and disappear later.

The non exact space and time coincidences between the maxima of magnetic field strength and brightness reported here cannot be explained by static flux tube models, like those presented by Spruit (1976) and subsequently by many other authors (Deinzer et al. 1984; Knölker et al. 1988; Knölker & Schüssler 1988; Grössmann-Doerth et al. 1989; Steiner & Pizzo 1989; Pizzo et al. 1993a, 1993b; Grössmann-Doerth et al. 1994; to refer to a few of them). In these models, the flux tubes are vertical and for a constant magnetic flux, both their brightness and field

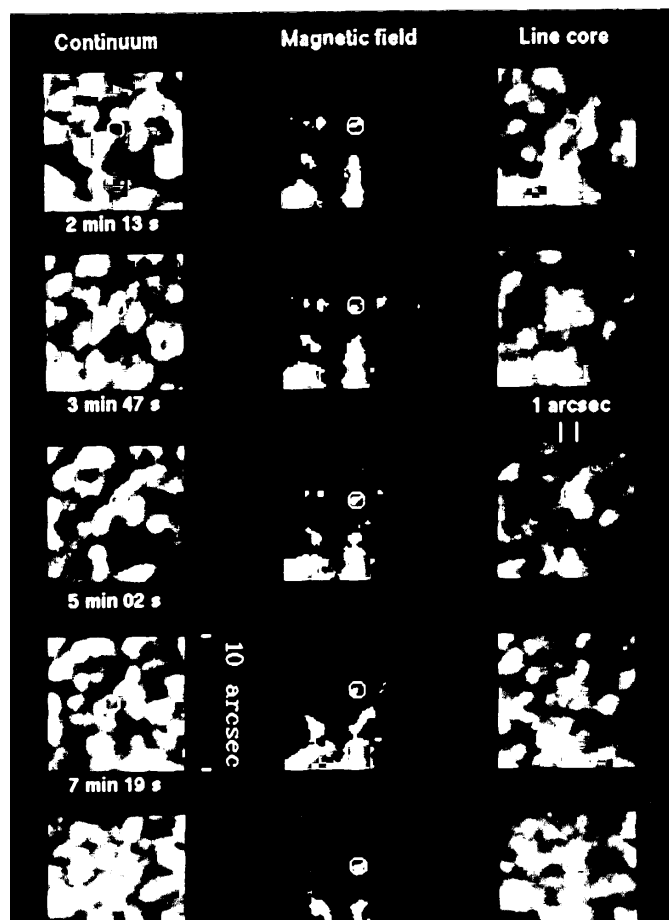


Fig. 4. A partial time series of magnetograms, with associated continuum and line core filtergrams, showing the appearance of a Network Bright Point at the junction of three granules (element *m* in Fig. 3). A magnetic flux is present in the space (at 2 min 13 sec) before the bright point appears (at 3 min 47 sec). The granules surrounding the dark space are converging, supposedly compressing the magnetic flux which becomes a bright flux tube

strength increase when the diameter decreases. Thus, maxima of brightness and field strength should coincide in time and space. Our observations should be considered in the frame of the dynamical 2-D model recently computed by Steiner et al. (1996; 1998), in which the flux tubes are allowed to be deformed by the dynamical surrounding granules, so that they can be inclined in the photosphere. When they are inclined, the longitudinal component of the magnetic field decreases like the cosine of the inclination angle; conversely the brightness increases because one sees better the hot wall of the tube. Another consequence of flux tube inclination is that the locations of the maxima of longitudinal field strength and of emergent intensity do not always coincide. It should be noted, however that 3-D models, like those computed by Nordlund and Stein, show much less flux tube bending than Steiner's 2-D model.

Among the 11 single bright points identified, only one appeared during the observation (labelled "*m*" in Fig. 3), but it has a particular interest. Part of its magnetic and intensity evolution

is shown in Fig. 4. A magnetic flux is present all over the time sequence, at the same position, with a 2σ threshold (0.5% of polarization); with a 2.5σ threshold, like in Fig. 3 b and c, this magnetic element is not always detected. At the beginning of the series, the magnetic field is located in a dark intergranular space, at the junction of three granules: there is no associated bright point visible in the continuum filtergram. A feature appears in this space at time $t = 3 \text{ min } 47 \text{ sec}$ ($t = 0$ is the beginning of our time series), while the three granules converge. This feature is visible in the following frames as an isolated point, which corresponds to a bright point in the line core: its size is about $0''.5$, which is nearly the average resolution of the observation. It is a typical case of Network Bright Point formation by granule compression, as described by Muller & Roudier (1992). It confirms the suggestion made by these authors that a magnetic flux is present in the intergranular space, prior to the appearance of the bright point, and that the converging granules play a role in the concentration and the brightening of the magnetic flux tube. The magnetic signal is too weak to permit any significant measurement of possible changes of field strength or flux. Apparently, the brightening appears in the line core before than in the continuum.

The present results, derived from a time series of interlaced magnetograms and filtergrams, in addition to those previously derived from wide band filtergrams of higher resolution (Muller 1983; Muller & Roudier 1992; Berger & Title 1996), support the suggestion, made by Muller & Roudier (1992), regarding the behavior of the magnetic flux elements embedded in the granular turbulent convection: they wander along the intergranular lanes, following the evolution of the local convection flow field. When the flow brings them into a dark space at the junction of converging granules, they are squeezed by these granules. As a consequence, their field strength increases as their cross-section decreases and they are partly evacuated; the gas remaining inside is heated by the hot walls of the magnetic elements, which have the shape of thin flux tubes; they brighten up and become visible as Bright Points in filtergrams. NBPs thus appear to be occasional brightenings of long-living flux tubes. They are often forced to split and merge under the action of the neighbouring granules.

Concerning the **bright points which are grouped** close together, they appear located inside a same magnetic area with an extension a little larger than that of the group of points (it is uneasy to define this extension precisely, because it depends on the threshold). Two such small areas are present in the selected field of view and are shown in Fig. 3. They have a dimension extending over $2''$ to $4''$ and contains respectively three NBPs (labelled a, b, d) and four NBPs (e, f, g, h). The resolution of the best magnetograms allows us to distinguish several maxima of magnetic signal in these areas, which coincide better than half an arcsecond with the positions of the associated NBPs. A permanent weaker signal is also detected between the evolving maxima, but when a bright point disappears, the magnetic surface loses an equivalent portion. A question then arises about the signal found in between the maxima: is it due to a real weaker field connecting strong flux tubes, or is it only some spread of

the signal, scattered in between the tubes by the instrument used and the processing applied to the observations? Such extended magnetic areas including several bright points have been observed previously by several authors (Keller 1992, 1995; Yi & Engvold 1993; Berger & Title 1996; Scharmer 1996), but they didn't point out the existence of several field strength maxima, corresponding to individual bright points.

6. Conclusions

In this work, individual magnetic elements have been resolved. Due to the homogeneous quality of the observations during the whole time series, some results have been found which are of help to understand the dynamics of flux tubes and their interactions with the solar granules. These can be summarized as follows.

The maximum magnetic signal V/I measured is 2.2% with a noise 0.25% rms, and the size of the smallest bright points is $0.5''$, or slightly less.

Every bright point, either isolated or belonging to a group, is associated with a magnetic element, and vice versa. However, the maxima of field strength and brightness do not necessarily occur at the same time. Furthermore, the position of the maximum magnetic field can be shifted relatively to the position of the maximum intensity by as much as $0.5''$.

There is one example of a magnetic element present at the beginning of the time series, which becomes bright only several minutes later, when it is compressed by the surrounding granules. This supports a suggestion made several years ago by Muller (1983) and subsequently by Muller & Roudier (1992), that an NBP corresponds to a temporary brightening of a persistent magnetic flux tube, which is forced by the granular flows to move at random along the intergranular lanes.

Our observations, so as recent ones by Berger & Title (1996), show that the concept of stable flux tube should be superseded by dynamical models like the one developed by Steiner et al. (1996).

When few Network Bright Points are clustered, the associated magnetic area is compact and extends beyond the group. Several maxima of field strength are visible in the patch and they correspond to the NBPs. The question subsists about the reality of the signal detected between these maxima.

There is, however, still much to learn about the fine structure of the magnetic field in the quiet Sun and its interaction with the convective flows, in order to understand some fundamental questions concerning: the origin of the flux tubes forming the photospheric network (are they generated by a local small-scale dynamo, or coming from active regions, swept by larger scale horizontal flows?); the generation of magneto-acoustic waves which could be able to heat the chromosphere and the corona; the relation between the network and the intranetwork magnetic features (which are one order of magnitude weaker, in term of flux); the latitude distribution of the magnetic flux outside active regions and its cycle dependence (this is important to understand the solar dynamo and the origin of the activity cycle). In order to solve these questions one needs long (several hours), homoge-

nous, high resolution (better than $0''5$) and high sensitivity time series of magnetograms (longitudinal and transversal) and filtergrams.

In order to try to meet these requirements we are working to improve the quality of the filter and will use in the future, a new fast CCD camera. However, not only high resolution, and high sensitivity, but also homogeneity is important to understand the magnetic field fluctuations which result from the interaction with the granulation. It is hard to get highly homogeneous time series of magnetograms, even under the best seeing conditions like those one can meet at the Pic du Midi Observatory (this work) or at La Palma (Keller 1992; Yi & Engvold 1993; Berger & Title 1996). It is even harder to get high resolution, homogeneous time series of spectroheliograms, which are of great interest because they contain more information about the magnetic and physical structure of the magnetic elements. One may expect to see some significant improvements in the near future, thanks to the use of fast, photometric CCD cameras, on one hand, and when the large aperture (90 cm), instrumental polarization free, THEMIS telescope will be operational, on the other hand. But if we really want to get long and homogeneous time series of high resolution magnetograms and spectroheliograms, one needs a telescope in space, able to reach $0''1$ of spatial resolution, during long periods of time. In order to be convinced one just have to look at the time series of magnetograms produced by SOHO/MDI, in its high resolution mode (resolution: $1''2$; pixel size: $0''6$; Title 1997; private communication).

Acknowledgements. We thank the technical staff at the Pic du Midi Observatory, in particular R. Dorignac, M. Fourcade, J. Gaye, P. Payssan, J. Rey, for the installation and adaptation of the Meudon Observatory filter magnetograph, on the Pic du Midi 50-cm refractor. We also thank L. November for having put to our disposal its image destretching code. The photographs have been digitized with the national microphotometer MAMA at Paris Observatory (Center for Images Analysis).

References

- Auffret H., Muller R., 1991, A&A 246, 264
 Berger T.E., Title A.M., 1996, ApJ. 463, 365
 Berger T.E., Schrijver C.J., Shine R.A., Tarbell T.D., Title A.M., Scharmer G., 1995, ApJ. 454, 531
 Bray R.J., Loughhead R.E., Durrant C.J., 1984, "The Solar Granulation", 2nd edition, Cambridge University Press, Cambridge.
 Chapman G.A., 1974, ApJ. 191, 255
 Deinzer W., Hensler G., Schüssler M., Weisshaar E., 1984, A&A 139, 435
 Del Toro Iniesta J.C., Semel M., Collados M., Sanchez Almeida J., 1990, A&A 227, 591
 Deubner F.L., 1989, in: Rutten R., Severino G. (eds.) Solar and Stellar Granulation, NATO Advanced Research Workshop, Capri, Italy, Kluwer, Dordrecht, p. 313
 Dollfus A., 1990, Solar Phys. 129, 1
 Dollfus A., Moity J., 1992, in "The Magnetic and Velocity Fields of Solar Active Regions", IAU Colloquium n° 141, Beijing, China
 Dollfus A., Colson F., Crussaire D., Launay F., 1985, A&A 151, 235
 Dollfus A., Crussaire D., Pernod E., Lioure A., 1986, C.R. Acad. Sc. Paris t. 303, Série II, n°2, 153
 Dunn R.B., Zirker J.B., 1973, Solar Phys. 33, 281
 Espagnet O., Muller R., Roudier Th., Mein N., Mein P., 1995, A&A Suppl. Ser. 109, 79
 Grossmann-Doerth U., Knölker M., Schüssler M., Weisshaar E., 1989, In Rutten R.J. and Severino G. (eds.) Solar and Stellar Granulation, Kluwer Dordrecht, p. 191.
 Grossmann-Doerth U., Knölker M., Schüssler M., Solanki S.K., 1994, A&A 285, 648
 Harvey J.W., Hall D., 1975, Bull. Amer. Astron. Soc. 7, 459
 Keller C.U., 1992, Nature 359, 307
 Keller C.U., 1995, In G. Klare (ed.) Reviews in Modern Astronomy, Vol. 8, Astronomical Gesellschafts, Hamburg.
 Keller C.U., Solanki S.K., Tarbell T.D., Title A.M., Stenflo J.O., 1990, A&A 236, 250
 Knölker M., Schüssler M., 1988, A&A 202, 275
 Knölker M., Schüssler M., Weisshaar E., 1988, A&A 194, 257
 Koutchmy S., 1977, A&A 61, 397
 Koutchmy S., Stellmacher G., 1978, A&A 67, 93
 Mehlretter J.P., 1974, Solar Phys. 38, 43
 Muglach K., Solanki S.K., 1992, A&A 263, 301
 Muller R., 1983, Solar Phys. 85, 113
 Muller R., 1985, Solar Phys. 100, 237
 Muller R., Keil S.L., 1983, Solar Phys. 87, 243
 Muller R., Mena B., 1987, Solar Phys. 112, 295
 Muller R., Roudier Th., 1992, Solar Phys. 141, 27
 Muller R., Roudier Th., Vigneau J., Auffret H., 1994, A&A 283, 232
 November L.J., 1986, Appl. Optics 25, 932
 Pizzo V.J., Mc Gregor K.B., Kunasz P.B., 1993a, ApJ. 404, 788
 Pizzo V.J., Mc Gregor K.B., Kunasz P.B., 1993b, ApJ. 413, 764
 Roudier Th., Espagnet O., Muller R., Vigneau J., 1994, A&A 287, 982
 Scharmer G., 1996, private communication
 Spruit H.C., 1976, Solar Phys. 50, 269
 Spruit H.C., Zwaan C., 1981, Solar Phys. 70, 207
 Stein R.F., Nordlund A., 1989, ApJ 342, L95
 Steiner O., Pizzo V.J., 1989, A&A 211, 447
 Steiner O., Pneuman G.W., Stenflo J.O., 1986, A&A 170, 126
 Steiner O., Grossmann-Doerth U., Knölker M., Schüssler M., 1995, In Klare G. (ed.) Reviews in Modern Astronomy, Vol. 8, Astronomical Gesellschafts, Hamburg.
 Steiner O., Grossmann-Doerth U., Schüssler M., Knölker M., 1996, Solar Phys. 164, 223, proceedings of an international Workshop on Solar Polarization, Stenflo J.O. and Nagendra K.N. (eds.)
 Steiner O., Grossmann-Doerth U., Knölker M., Schüssler M., 1998, ApJ. 495, 468
 Stenflo J.O., 1973, Solar Phys. 32, 41
 Stenflo J.O., Solanki S.K., Harvey J.W., 1987, A&A 173, 167
 Stolpe F., Kneer F., 1997, A&A 317, 942
 Tarbell T.D., Title A.M., 1997, Solar Phys. 52, 13
 Title A.M., 1997, Private communication
 Title A.M., Berger T.E., 1996, ApJ. 463, 797
 Title A.M., Tarbell T.D., Simon G.W. and the SOUP Team: 1986, Adv. Space Res. 61 (8), 253
 Title A.M., Tarbell T.D., Topka K.P., Ferguson S.H., Shine R.A. and the SOUP Team: 1989, ApJ. 336, 475
 Title A.M., Topka K.P., Tarbell T.D., Schmidt W., Balke Ch., Scharmer G., 1992, ApJ. 393, 782
 Yi Z., Engvold O., 1993, Solar Phys. 144, 1
 Zayer I., 1990, Ph. D. Thesis, ETH Zürich
 Zayer I., Solanki S.K., Stenflo J.O., 1989, A&A 211, 463